

following expression for the branching fraction

$$\frac{k_B}{k_X} = \frac{\sum_{v_1 v_2} [E_B - (G_{v_1} + G_{v_2}^B)]^{5/2} (B_{v_1} B_{v_2}^B)^{-1}}{\sum_{v_1 v_2} [E_X - (G_{v_1} + G_{v_2}^X)]^{5/2} (B_{v_1} B_{v_2}^X)^{-1}} \quad (13)$$

where E_B (calculated as 10 203 cm^{-1}) and E_X (calculated as 40 709 cm^{-1}) are the total translational, vibrational, and rotational energy of the product channel corresponding to the NS(B) and NS(X) states, respectively.³⁴ G_{v_1} , $G_{v_2}^X$, and $G_{v_2}^B$ are the vibrational terms²¹ for the species $\text{N}_2(\text{X})$, NS(B), and NS(X), respectively. Similarly, B_{v_1} , $B_{v_2}^B$, and $B_{v_2}^X$ are the rotational terms²¹ for the species $\text{N}_2(\text{X})$, NS(B), and NS(X), respectively. The summation is taken over all vibrational levels for species v_1 (taken as N_2) and v_2 (taken as NS) for which the quantities in the brackets remain real. Using the known spectroscopic terms for N_2 and NS and the calculated values of E_B and E_X , we obtain an estimated branching ratio of 0.0051 for eq 13. Since the statistical prediction of the branching fraction for this reaction is small and thus consistent to what was obtained experimentally, the energy disposal into the product channels appears to be statistical in nature and reflects the large number of mixed surfaces available to the $\text{S} + \text{N}_3$ reaction. The lack of a dynamical constraint in the $\text{S} + \text{N}_3$ reaction can be compared to other atom reactions with azide radicals such as the $\text{N}(^4\text{S}) + \text{N}_3(\text{X}^2\Pi) \rightarrow \text{N}_2(\text{B}^3\Pi) + \text{N}_2(\text{X}^1\Sigma^+)$ reaction. Strong spin and orbital angular momentum constraints are cited^{13a} in this reaction to account for the relatively high (>20%) photon yield of $\text{N}_2(\text{B})$.

Our initial interpretation of the origin of the bimodal component in the rotational distribution of NS(B) at lower pressures was to

(34) E_B and E_X are calculated from the following expression given in ref 33, $E = E_T + E_{\text{mol}} - D_0^\circ(\text{N}_3) + D_0^\circ[\text{NS}(\text{X})] - T_0$. E_T is the reactant relative translational energy, E_{mol} is the average internal energy of N_3 and is calculated from a classical rigid rotor and known vibrational frequencies^{34a} of N_3 ($\nu_3 = 2041 \text{ cm}^{-1}$, $\nu_{\text{as}} = 1344 \text{ cm}^{-1}$, $\nu_{\text{bend}} = 500 \text{ cm}^{-1}$) at 300 K, $D_0^\circ(\text{N}_3)$ is the bond dissociation energy ($\approx 1 \text{ kcal mol}^{-1}$)^{34b} of the N–N₂ bond in N_3 , $D_0^\circ[\text{NS}(\text{X})]$ is the bond dissociation energy^{34c} of NS and is taken as 38 717 cm^{-1} , and T_0 is the electronic term^{34c} of the NS($\text{B}^2\Pi_{1/2}$) state, 30 085 cm^{-1} . Since there is considerable uncertainty in the bond dissociation energy of the N–N₂ bond, E_B and E_X are only estimated values. (a) Patai, S., Ed. *The Chemistry of the Azido Group*; Interscience: London, 1971. (b) Reference 29. (c) Reference 21.

assign it to a collisional process whereupon collisions relax upper J levels of a residual nascent distribution such that the true nascent distribution may consist of a single rotational envelope. However, one cannot exclude the possibility of direct and complex mode reaction dynamics from occurring in this reaction. For example, Breckenridge and co-worker³⁵ report the occurrence of direct and complex reaction modes in the bimodal rotational distribution resulting from the $\text{Mg}(\text{P}_1) + \text{H}_2 \rightarrow \text{MgH}(\nu, J) + \text{H}$ reaction. It was stated that a direct H atom abstraction accounts for the rotational distribution for low J levels and an insertion reaction followed by HMgH complex dissociation for the high J component. Further, Obase et al.³ interpreted the dynamics of the $\text{N}(^2\text{D}) + \text{OCS} \rightarrow \text{NS}(\text{B}^2\Pi) + \text{CO}$ reaction in terms of a direct mode by comparing the nascent NS(B) product distributions to that predicted from a prior distribution. Whether the $\text{S} + \text{N}_3$ reaction occurs through a direct or complex mode is not ascertainable with the current data.

Summary and Conclusions

The $\text{S}(^3\text{P}) + \text{N}_3(\text{X}^2\Pi)$ reaction has been studied as a source of NS($\text{B}^2\Pi$) chemiluminescence in the 290–520-nm range. The rate constant for this reaction was measured and found to be $(3.5 \pm 0.9) \times 10^{-11} \text{ cm}^3 \text{ s}^{-1}$ with an NS($\text{B}^2\Pi$) yield of 0.06%. The steady-state NS(B) vibrational distribution formed was found to be non-Boltzmann. An empirically determined NS($\text{B}^2\Pi$) rotational distribution can be fit to the sum of a Boltzmann distribution with an effective rotational temperature of 1200 K combined with a Boltzmann-like distribution that takes effect for J levels ≥ 50 . The yield of NS(B) was interpreted as being a function of the potential energy surfaces available to the reactants and products. Since the $\text{S} + \text{N}_3$ reaction possesses a large number of surfaces available and weak angular momentum correlations prevail in this reaction, the energy disposal into electronic excitation is small and is statistical in nature. By comparison, the high yield (>20%) of $\text{N}_2(\text{B}^3\Pi)$ from the $\text{N}(^4\text{S}) + \text{N}_3(\text{X}^2\Pi)$ reaction^{13a} was attributed to the strength of the spin and orbital angular momentum constraints in that system.

Registry No. NS, 12033-56-6; S, 7704-34-9; N_3 , 14343-69-2.

(35) See for example: Breckenridge, W. H. In *Reactions of Small Transient Species, Kinetics and Energetics*; Fontijn, A., Clyne, M. A. A., Eds.; Academic Press: New York, 1983.

Photophysical Properties of Methylated Phenols in Nonpolar Solvents

G. Grabner,* G. Köhler,

Institut für Theoretische Chemie und Strahlenchemie der Universität Wien, Währingerstrasse 38, A-1090 Wien, Austria

G. Marconi,* S. Monti, and E. Venuti

Istituto F.R.A.E.-C.N.R., Via de'Castagnoli 1, I-40126 Bologna, Italy (Received: July 11, 1989; In Final Form: November 22, 1989)

The photophysical properties of phenol and a series of mono-, di-, and trimethyl-substituted phenols excited in their first singlet state in hydrocarbon solvents have been investigated by measuring fluorescence lifetimes and quantum yields and lowest triplet and phenoxy radical formation quantum yields. The compounds studied have small quantum yields for fluorescence ($\phi_F = 0.02$ – 0.075) and higher ones for triplet formation ($\phi_T = 0.05$ – 0.35) and O–H bond photodissociation ($\phi_R = 0.08$ – 0.21), but in all cases the sum $\phi_F + \phi_T + \phi_R$ is smaller than 0.5. The nature of the radiationless deactivation processes involving the lowest singlet and triplet states, and the influence of ring methylation upon them, are discussed in light of the results. The importance of a triplet pathway in the photodissociation is confirmed.

Introduction

The family of phenols and related molecules presents a variety of interesting features when excited into the lowest excited states. These phenomena include energy-dependent fluorescence quantum yield,^{1,2} O–H bond dissociation,^{2,3} and electron ejection in polar

solvents.^{4,5} The latter features are particularly important from the point of view of the behavior of the aromatic amino acid

(1) Köhler, G.; Getoff, N. *Chem. Phys. Lett.* **1974**, *26*, 525.

(2) Köhler, G.; Getoff, N. *J. Chem. Soc., Faraday Trans. 1* **1976**, *72*, 2101.

tyrosine and tyrosine-containing proteins.⁶

In the past years, we investigated the photophysical properties of phenol and anisole in nonpolar solvents by measuring fluorescence and triplet quantum yields,⁷ as well as temperature⁸ and isotope⁹ effects on the fluorescence lifetimes. From the study of the photophysical parameters derived from these experiments and by means of a theoretical model based on semiempirical calculations, we were able to propose a mechanism of deactivation of the lowest singlet states of phenol in nonpolar solvents. This mechanism implies the presence of a low-lying dissociative triplet curve, which crosses the singlet potential energy curve at different energies giving rise to different dissociation rates when the molecule is excited in either S_1 or S_2 .

In this paper, we extend this kind of photophysical investigation to the methylated compounds, i.e., to the family of cresols [2-, 3-, and 4-methylphenol (2-, 3-, and 4-MP)] and to some dimethylated [3,5-, 2,4-, and 2,6-dimethylphenol (3,5-, 2,4-, and 2,6-DMP)] as well as trimethylated phenols [2,3,5- and 2,4,6-trimethylphenol (2,3,5- and 2,4,6-TMP)]. Only processes occurring upon excitation in S_1 will be dealt with. It is known that methyl substitution causes both inductive and mesomeric effects¹⁰ on the excited states of aromatic compounds, which influence the spectral properties of the molecules. Moreover, the photophysical properties of the substituted compounds can be related to those of the unsubstituted parent and analyzed in terms of perturbed energy levels and absorption coefficients.

A further aim of the present work was to put these model considerations on a firmer experimental basis. To that end, measurements of fluorescence lifetimes and quantum yields have been supplemented with experimental determination of the quantum yields for the formation of the lowest triplet state on the one hand and of phenoxyl radicals on the other, by transient absorption spectroscopy. Heavy-atom quenching experiments on 2-methylphenol have also been carried out.

Experimental Section

Phenol and methyl-substituted phenols (Aldrich) were purified by repeated sublimation in a dry nitrogen atmosphere. In order to prevent formation of hydrogen bonds between the phenols and water present in the solvent, care was taken to purify and dehydrate the solvent 3-methylpentane used in the temperature-dependent fluorescence experiments. The relevant procedures have been described.⁹ The solvent *n*-hexane (Merck, for fluorescence spectroscopy) and the heavy-atom quencher 1-bromobutane (Aldrich, "Gold Marke") were used without further purification. All these substances were nonfluorescent.

Experimental procedures for measurement of fluorescence lifetimes and emission spectra have been described previously.⁹ Anisole in *n*-hexane was chosen as a standard for the determination of absolute quantum yields at 293 K and $\lambda_{exc} = 275$ nm.

Quantum yields of triplet and radical formation were measured by laser flash photolysis. A frequency-quadrupled Nd:YAG laser (Quanta-Ray DCR-1) was used for excitation at $\lambda = 266$ nm. A right-angle geometry of analyzing and exciting beams, delimited by rectangular apertures, was used to determine light fluxes (measured with a Raycon-Wec 730 ballistic calorimeter) and photoproduct absorbances in a controlled geometry. Optical path lengths of exciting and analyzing light beams in the probed cell volume were 0.17 and 0.32 cm, respectively. All measurements were made at laser pulse energies kept as low as possible (<1.5 mJ/pulse for radical and triplet-triplet absorption studies, <0.1

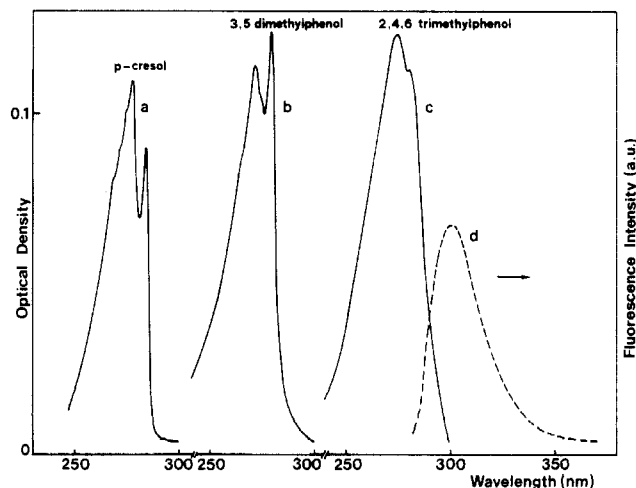


Figure 1. Absorption spectra of 2-MP (a), 3,5-DMP (b), and 2,4,6-TMP (c) and typical unstructured emission spectrum of a methylated phenol in 3-methylpentane. Concentrations are around 5×10^{-5} M.

TABLE I: Experimental Deactivation Parameters of Phenol and Methylated Phenols in Nonpolar Solvent (3-Methylpentane or *n*-Hexane)

compd	τ_F^a	ϕ_F^b	ϕ_T^b	ϕ_R^b	$1 - (\phi_F + \phi_T + \phi_R)$
phenol	2.3	0.075	0.24	0.13	0.555
2-MP	1.6	0.042	0.10	0.18	0.68
3-MP	2.1	0.051	0.21	0.14	0.59
4-MP	2.5	0.065	0.35	0.08	0.505
2,6-DMP	1.9	0.060	0.12	0.21	0.61
2,4-DMP	1.8	0.035	0.18		
3,5-DMP	2.1	0.065	0.19	0.14	0.605
2,4,6-TMP	2.1	0.075	0.21	0.20	0.525
2,3,5-TMP	0.66	0.020	0.05	0.18	0.768

^a Instrument accuracy: ± 0.1 ns. ^b Estimated accuracies: ϕ_F , $\pm 10\%$; ϕ_T , $\pm 10\%$; ϕ_R , $\pm 20\%$.

mJ/pulse for energy-transfer studies; 1 mJ/pulse equivalent to 3.2×10^{16} photons/cm²) to minimize heating effects and errors due to second-order reactions. Extensive signal averaging (over up to 512 pulses) was used for signal-to-noise ratio enhancement. The temperature was 295 ± 2 K. Energy transfer to anthracene¹¹ was used to measure the quantum yields for the formation of the lowest triplet states of phenol and methylated phenols in *n*-hexane. The results are based on $\phi_T = 0.7$ for anthracene.¹² Phenol concentrations between 3×10^{-4} and 4×10^{-3} M and anthracene concentrations between 8.6×10^{-5} and 4.3×10^{-4} M were used, without influence of these concentrations on the results. Highest corrections for triplet formation by direct excitation of anthracene amounted to 60%. Small monochromator bandwidths (<0.3 nm) and frequent checks of wavelength setting were performed in order to keep errors induced by the narrow half-width of the anthracene triplet-triplet absorption at 420 nm small.

Phenoxyl radical spectra were measured with monochromator bandwidths smaller than 0.2 nm. No correction for the slit function was made. Band half-widths and peak wavelengths were determined by fitting a Gaussian function to the experimental data.

Calculations were performed using the CNDO/S¹³ program including singly and doubly excited configurations in a space of 80 configurations previously tested.¹⁴

Results

Absorption and Fluorescence Properties. The S_0 - S_1 spectra of methylated phenols extend from 260 to 300 nm with extinction coefficients of the same order as those of unsubstituted phenol

(3) Zechner, J.; Köhler, G.; Grabner, G.; Getoff, N. *Can. J. Chem.* **1980**, *58*, 2006.

(4) Grabner, G.; Köhler, G.; Zechner, J.; Getoff, N. *Photochem. Photobiol.* **1977**, *26*, 449.

(5) Grabner, G.; Köhler, G.; Zechner, J.; Getoff, N. *J. Phys. Chem.* **1980**, *84*, 3000.

(6) Creed, D. *Photochem. Photobiol.* **1984**, *39*, 563.

(7) Köhler, G.; Kittel, G.; Getoff, N. *J. Photochem.* **1982**, *18*, 19.

(8) Dellonte, S.; Marconi, G. *J. Photochem.* **1985**, *30*, 37.

(9) Dellonte, S.; Marconi, G.; Monti, S. *J. Photochem.* **1987**, *39*, 33.

(10) Salem, L. *The Molecular Orbital Theory of Conjugated Systems*; W.A. Benjamin: Reading, MA, 1966; Chapter 7.

(11) Klein, R.; Tatischeff, I.; Bazin, M.; Santus, R. *J. Phys. Chem.* **1981**, *85*, 670.

(12) Amand, B.; Bensasson, R. *Chem. Phys. Lett.* **1975**, *34*, 44.

(13) Del Bene, J.; Jaffé, H. H. *J. Chem. Phys.* **1968**, *48*, 1807.

(14) Del Bene, J.; Jaffé, H. H. *J. Chem. Phys.* **1968**, *49*, 1221.

TABLE II: Spectral Parameters of Phenoxyl and Methylated Phenoxyl Radicals

compd	solvent H ₂ O			solvent <i>n</i> -hexane			
	λ_{\max}^a , nm	$\Delta\lambda_{1/2}^b$, nm	ϵ_{\max}^a , M ⁻¹ cm ⁻¹	λ_{\max}^a , nm	$\Delta\lambda_{1/2}^b$, nm	ϵ_{\max}^a , M ⁻¹ cm ⁻¹	$\epsilon\phi^a$, M ⁻¹ cm ⁻¹
phenol	400.3	9.1	3000	399.0	8.7	3140	398
2-MP	394.9	8.5	2760	394.4	8.0	2930	526
3-MP	411.1	10.6	3250	407.6	8.7	3960	573
4-MP	405.5	10.2	4940	403.0	9.8	5140	432
2,6-DMP	389.8	8.95	2360	390.4	8.8	2400	514
3,5-DMP	427.4	13.8	3570	419.7	9.1	5410	734
2,4,6-TMP	396.3	10.3	3970	395.0	9.9	4130	831
2,3,5-TMP	419.2	15.95	2985	411.8	10.5	4530	828

^a Estimated accuracies: λ_{\max} , ± 1 nm; $\epsilon_{\max}(\text{H}_2\text{O})$, $\pm 5\%$; $\epsilon_{\max}(n\text{-hexane})$, $\pm 10\%$; $\epsilon\phi(n\text{-hexane})$, $\pm 10\%$. ^b Statistical error as determined by changing the wavelength interval of a Gaussian fit: ± 0.3 nm.

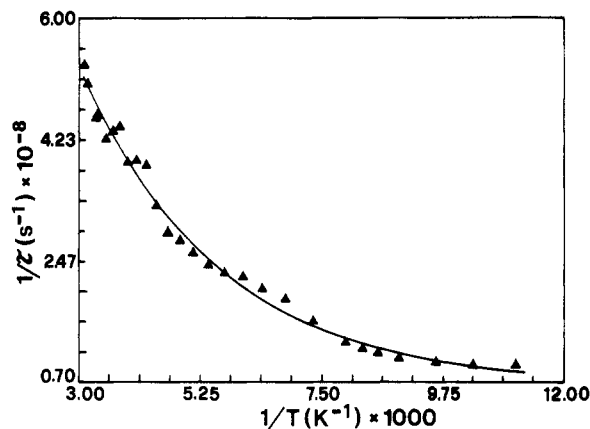


Figure 2. Behavior of the reciprocal lifetime of 2,4,6-TMP as a function of $1/T$. The full curve was calculated by fitting eq 1 to the experimental points.

(around 2000 M⁻¹ cm⁻¹ at the absorption maximum). This indicates that the electronic transition has the same nature and is only slightly perturbed by methylation. In a 3-methylpentane solution, with an instrumental resolution of 2 nm and concentrations of about 5×10^{-5} M, the vibrational structure of the spectra seems to be dependent on the substituent position. As examples, we report in Figure 1 the absorption spectra of 2-MP, 3,5-DMP, and 2,4,6-TMP.

The emission spectra are in all cases unstructured and peak around 290–300 nm (see spectrum d in Figure 1). The fluorescence lifetimes, τ_F , in 3-methylpentane and the quantum yields, ϕ_F , obtained by excitation in S_1 ($\lambda_{\text{exc}} = 275$ nm) are reported in Table I.

Some of the lifetimes and quantum yields were also determined in *n*-hexane solutions; no significant deviations from the results in 3-methylpentane were observed. The temperature dependence of the fluorescence lifetime of 4-MP and 2,4,6-TMP was measured between 90 and 320 K by exciting in the first singlet state. Figure 2 shows the behavior of the reciprocal lifetimes of 2,4,6-TMP as a function of $1/T$.

The continuous curve was calculated by a nonlinear least-squares procedure using the following law:

$$k = k_0 + A \exp(-\Delta E/RT) \quad (1)$$

The values obtained for k_0 , A , and ΔE are 6.5×10^7 s⁻¹, 1.5×10^9 s⁻¹, and 0.8 kcal/mol for 2,4,6-TMP and 1.3×10^8 s⁻¹, 5.5×10^9 s⁻¹, and 1.7 kcal/mol for 4-MP. All of these parameters are of the same order of magnitude as the corresponding ones previously determined for phenol and its deuterated derivatives.^{8,9}

Triplet-State Properties. In aqueous solution, phenol and methylated phenols exhibit a broad, unstructured triplet-triplet absorption extending into the visible.^{15,16} Extinction coefficients are not known with certainty but are probably rather low (<1000 M⁻¹ cm⁻¹ for $\lambda > 300$ nm), which makes the measurement of triplet-triplet absorption difficult. Triplet lifetimes observed under

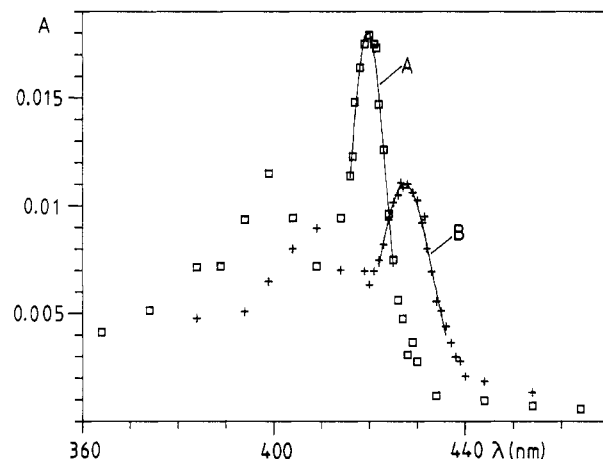


Figure 3. Spectra of 3,5-dimethylphenoxyl radicals obtained from 10^{-3} M 3,5-DMP at 1 mJ/pulse: (A) *n*-hexane, plus 10^{-3} M 2,4-hexadiene, saturated with argon; (B) H₂O, pH 12.3, plus 0.2 M *tert*-butyl alcohol, saturated with N₂O. Solid curves were obtained from a Gaussian fit.

conditions of pulsed laser excitation are of the order of a few microseconds.¹⁵ These observations apply also to *n*-hexane solutions; here, too, a weak transient absorption, sensitive to triplet quenchers such as O₂ and 2,4-hexadiene, is detectable and assigned to triplet-triplet absorption. Figure 5 (see below) shows an example of the time course of this transient at $\lambda = 430$ nm in the case of phenol.

The quantum yields for triplet formation of phenol and methylated phenols in *n*-hexane, determined by energy transfer to anthracene, are also presented in Table I. A value of $\phi_T = 0.32$ was previously found for phenol in cyclohexane by a steady-state method.⁷

Photodissociation. Steady-state photoproduct analysis shows OH bond cleavage to be the main photochemical process occurring upon excitation of phenol and methylated phenols in nonpolar solvents.² By use of H atom scavengers, substantial H₂ quantum yields are obtained even when the compounds are excited in their first singlet state, in contrast to polar solutions (ethanol or H₂O), where H₂ yields are very low in these conditions.³

Flash photolysis of phenols results in the formation of phenoxyl radicals both in polar and nonpolar media.¹⁷ These radicals are easily observed by transient absorption spectroscopy owing to their characteristic double-band spectrum with the main peak lying around 400 nm. Measurement of phenoxyl radical formation can therefore be used to determine OH bond cleavage quantum yields, provided the extinction coefficients of the radicals are known. This is not the case in nonpolar solutions, but a convenient measurement can be made in alkaline aqueous solution (i.e., with phenols in dissociated form); here hydrated electrons, the extinction coefficients of which are accurately known, are the only photochemical products along with their counterpart phenoxyl radicals. This process is monophotonic,¹⁸ in contrast to phenoxyl radical for-

(15) Bent, G.; Hayon, E. *J. Am. Chem. Soc.* **1975**, *97*, 2599.

(16) Grabner, G. *Proc.—IUPAC Symp. Photochem. 11th* **1986**, 129.

(17) Land, E. J.; Porter, G. *Trans. Faraday Soc.* **1963**, *59*, 2016, 2027.
(18) Feitelson, J.; Hayon, E.; Treinin, A. *J. Am. Chem. Soc.* **1973**, *95*, 1025.

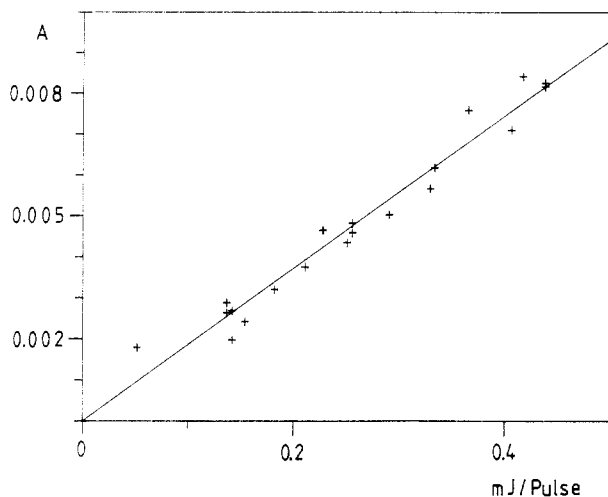


Figure 4. Dependence of absorbance at 420 nm on laser pulse energy for radicals obtained from 10^{-3} M, 3,5-DMP in hexane. Solid line represents a least-squares fit.

mation from undissociated phenols in polar solutions, which is dominated by two-photon processes at high excitation intensities.⁴

Determination of phenol photodissociation quantum yields, ϕ_p , by a transient absorption method in *n*-hexane thus requires a comparison of the spectral properties of the radicals in this solvent on the one hand and in alkaline water on the other. This is done in Table II and Figure 3.

Phenoxy radical spectra are rather similar in the two solvents, but there are characteristic differences. Most pronounced is a red shift and broadening of the absorption in water when a methyl group is introduced in the meta position; the origin of this effect is not known. As an example, Figure 3 shows the spectra of 3,5-dimethylphenoxy radicals in *n*-hexane and water (pH 12.3). Also shown are the results of the Gaussian fit to the experimental data. As can be seen from Table II, these differences are much less pronounced for substitution in ortho or para positions. Extinction coefficients presented in Table II for *n*-hexane solutions are deduced from those determined in alkaline water as described above by assuming that they are inversely proportional to the band half-widths.

Figure 4 shows the dependence of the transient absorbance at the pulse end due to the 3,5-dimethylphenoxy radical in *n*-hexane on laser pulse energy. Radical absorption is easily distinguishable from triplet-triplet absorption at low pulse energy due to the much longer lifetime of the former.

The linear relationship obtained indicates that OH bond dissociation is a purely one-photon process in nonpolar solution. This behavior was observed for all phenols studied. The determination of the product of extinction coefficient and quantum yield is thus possible. These results are also included in Table II. The photodissociation quantum yields ultimately obtained are included in Table I. H_2 yields previously determined by H atom scavenging at $\lambda_{exc} = 254$ nm for phenol (0.12), 3,5-DMP (0.14), and 2,4,6-TMP (0.13) in cyclohexane² are in good agreement with the present ones.

Further experiments were conducted to investigate possible pathways leading to phenoxy radicals. Figure 5 shows the course of radical and triplet-triplet absorption from phenol in *n*-hexane in the first microseconds after the laser pulse.

Addition of the triplet quencher 2,4-hexadiene gives, at 400 nm, transient B which has a lower absorbance than transient A in the first few microseconds. The difference is attributed to triplet-triplet absorption. At 430 nm, the phenoxy radical does not absorb and only T-T absorption is present (transient C). Addition of 2,4-hexadiene eliminates all transients at 430 nm. Accordingly, by combining the transients in the form

$$D = A - (\epsilon_{TT}(400)/\epsilon_{TT}(430))C - B \quad (2)$$

the time course of possible radical formation from the lowest relaxed triplet state (T_1^0) is obtained. Figure 5 demonstrates that

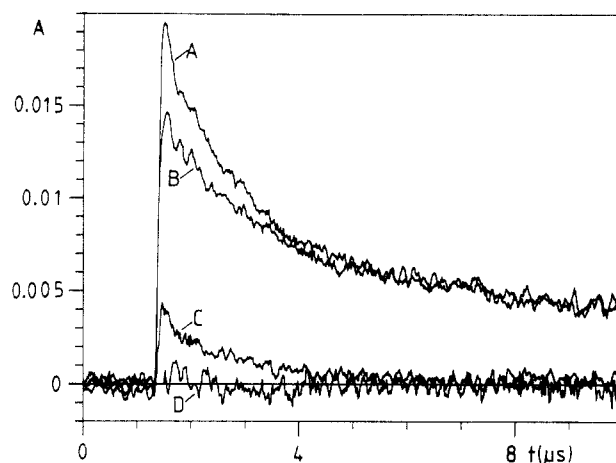


Figure 5. Time course of absorption of phenol triplets and phenoxy radicals obtained from 3.35×10^{-3} M phenol in *n*-hexane, saturated with argon, at 1.05 mJ/pulse: (A) 400 nm, without additives; (B) 400 nm, plus 10^{-3} M 2,4-hexadiene; (C) 430 nm, without additives; (D) absorbance calculated according to eq 2.

TABLE III: Influence of the Concentration, [Q], of the Heavy-Atom Quencher 1-Bromobutane on Deactivation Parameters of 2-MP in *n*-Hexane

[Q], M	τ_F , ^a ns	ϕ_T	ϕ_R	$(\phi_T/\tau_F)/(\phi_T/\tau_F)_0$	$(\phi_R/\tau_F)/(\phi_R/\tau_F)_0$
0	1.4	0.10	0.18	1	1
0.25	1.05	0.15	0.217	2.0	1.6
0.5	0.84	0.22	0.222	3.7	2.1
1	0.60	0.30	0.257	7.0	3.3

^a Calculated from quenching constant, $k_q = 9.4 \times 10^8$ M⁻¹ s⁻¹.

no radicals are produced in this way.

Additional information is obtained from the effect of O₂ saturation on fluorescence and radical yields. By use of 2,4,6-TMP in *n*-hexane as a model compound, a reduction in radical formation to 0.44 of its value in O₂-free solution was found upon saturation with O₂. In the same conditions, fluorescence is reduced to 0.42 of its value in O₂-free solution.

Heavy-Atom Effect on Deactivation of Excited 2-MP. Like related Br-containing molecules,^{19,20} 1-bromobutane can be expected to enhance intersystem crossing. Experimentally, it is found to be an efficient fluorescence quencher, the quenching constant being $k_q = 9.4 \times 10^8$ M⁻¹ s⁻¹. In contrast, the fluorescence lifetime of 2-MP is slightly increased to $\tau_F = 1.7$ ns by addition of 2 M 1-chlorobutane; this effect may be ascribed to a change in solvent polarity. Quenching by 1-bromobutane is thus likely to proceed by heavy-atom perturbation.

1-Bromobutane is reasonably well suited for pulsed laser measurements at $\lambda_{exc} = 266$ nm since it has a low extinction coefficient ($\epsilon = 0.4$ M⁻¹ cm⁻¹) at this wavelength. Laser excitation of 1-bromobutane in *n*-hexane produces a short-lived transient with an absorption maximum around 360 nm which decays in a rapid first-order reaction ($k = 2 \times 10^6$ s⁻¹). This transient interacted neither with 2-MP, as shown by measurements at varying 2-MP concentrations, nor with O₂ and was not further investigated.

Table III shows the results of measurements of τ_F , ϕ_T , and ϕ_R obtained at quencher concentrations, [Q], between 0 and 1 M. ϕ_T was determined by recording the triplet-triplet absorption at 430 nm and assuming that its extinction coefficient is not influenced by addition of 1-bromobutane. ϕ_R was obtained from the radical absorption at 392.5 nm, which at low excitation intensities (0.1 mJ/pulse or lower) is easily distinguished from the 1-bromobutane transient by its much longer lifetime (~ 50 μ s).

The results of Table III show that both ϕ_T and ϕ_R increase with increasing [Q], but radical formation is less enhanced than triplet formation.

(19) Medinger, T.; Wilkinson, F. *Trans. Faraday Soc.* **1965**, *61*, 620.
(20) Jardon, P. *J. Chim. Phys.* **1975**, *72*, 52.

Discussion

In order to discuss the deactivation pathways of the S_1 state of phenol and methylated phenols in nonpolar solvents, we have four independent experimental data, reported in Table I, namely, the fluorescence lifetimes and quantum yields (τ_F , ϕ_F) and the efficiencies of formation of the relaxed triplet state T_1^0 (ϕ_T) and of the free phenoxyl radical R^* (ϕ_R). In the same table the quantities $1 - (\phi_F + \phi_T + \phi_R)$ are also reported.

We note that methylation does not induce strong differences in τ_F values, which remain around 2 ns in all the derivatives. An exception is represented by 2,3,5-TMP which has a considerably faster deactivation rate. The radiative channel seems to be by far the less important accounting for no more than 8% of the S_1 decay.

$S_1 \rightsquigarrow T_1$ intersystem crossing is more significant. This is in agreement with the temperature dependence of the total decay rate parameter. As already reported for phenol,^{8,9} the relatively low values of the preexponential factors in the Arrhenius dependence of $1/\tau_F$ versus $1/T$ (Figure 2) clearly suggest the occurrence of a spin-forbidden process in the S_1 deactivation. ϕ_T grossly correlates with ϕ_F but is, however, much lower than in polar solvents ($\phi_T = 0.65$ for phenol in ethanol) and does not represent the main nonradiative process of S_1 .

The efficiency of the dissociative channel is assumed to be of the order of ϕ_R even if, in principle, it could be higher due to the possibility of cage recombination of the radical fragments (R^* , H^*). The possible importance of fragment recombination is difficult to assess in the case of phenol photodissociation. In nonviscous solvents, rotational relaxation motions are expected to change the relative orientation of the fragments in times comparable to dissociative relaxation. For example, excited aniline in isopentane has been reported to undergo inertial ("free") rotation with relaxation times of the order of 1 ps before interacting with solvent molecules.²¹ On the other hand, the delocalized nature of the electron distribution in the phenoxyl radical allows for several sites of H atom attack, namely, the oxygen atom and the ortho and para carbon atoms.²² This situation is not changed much by methylation.²³

Assuming that recombination is negligible, the last column in Table I represents the yields of all the remaining nonradiative processes starting from S_1 . Recent literature²⁴⁻²⁶ on the behavior of supersonic jet cooled molecules has established that the rate of internal conversion from S_1 to the ground state is much more important in free phenol than in the phenol-H₂O complex, suggesting that the OH stretch is the dominant accepting mode. This has been confirmed by the presence of a strong deuterium isotope effect on the S_1 lifetime.²⁷ (It has to be noted that the deuterium effect reported in ref 27 is by far larger than that detected by us in solution.⁹ The origin of this discrepancy is not clear at the moment.) On the basis of these findings, the last column in Table I could be attributed to internal conversion. These values are in general larger than 0.5 so that nonradiative decay to S_0 could be the dominant channel deactivating S_1 in nonpolar solvents. Since the OH stretching mode appears to be the most important mode in the radiationless deactivation of S_1 , it is expected that differences

in the Franck-Condon factors involving this vibration can be effective in differentiating the conversion process $S_1 \rightsquigarrow S_0$ and, consequently, the lifetimes of the methylated compounds. In order to investigate this problem, we performed a series of semiempirical calculations (CNDO/S and INDO/S, including singly and doubly excited configurations) without obtaining any evident correlation between the calculated energy gaps and the experimental lifetimes. We feel, therefore, that more refined calculations, including geometry optimization in S_1 , are necessary in order to gain insight into the problem of the internal conversion in these compounds. In fact, a correlation recently found between the $pK_a(S_1)$ and the position of the substituents in a series of bimethylated phenols²⁸ supports the idea that the geometry of the OH bond is especially affected in S_1 by methylation on the ring. Finally, the presence of an important radiationless process competing with intersystem crossing is confirmed by the strong heavy-atom-induced increase of ϕ_T in 2-MP in the presence of 1-bromobutane (Table III). Keeping in mind that the results of the heavy-atom experiments must be considered as preliminary in the sense that further studies are needed to ascertain the nature of the fluorescent state, we observe that the extent of increase in ϕ_T is in agreement with the expected effect of an external heavy atom in strongly fluorescent molecules.²⁹

Let us now consider the photodissociative process. The effect of oxygen on the yield of radicals and fluorescence suggests that no photodissociation takes place prior to relaxation to the fluorescent state and that, if O₂ quenching leads to the population of the lowest triplet, it does not produce additional radicals. In agreement with this fact, Figure 5 demonstrates that no radicals are formed from the relaxed triplet state T_1^0 . Furthermore, by comparing in Table I the values of ϕ_T and ϕ_R within the different groups of derivatives, we observe that there is a negative correlation between the two quantities. On the other hand, the heavy-atom-induced increase of the 2-MP radical yield, reported in Table III, does not parallel the extent of the increase of the triplet yield. These results unequivocally demonstrate the importance of the triplet manifold in the photodissociation. However, the previously proposed model,⁹ involving a vibrationally excited level of T_1 as a common precursor both to dissociation and to lowest triplet formation, cannot easily be reconciled with the present results.

Any further conclusion must remain tentative. The results could point to a mechanism involving two independent intersystem crossing steps, but mechanisms requiring more than one dissociative channel could also be operating. Preference for a mechanism of triplet character rests mainly on the argument that dissociative singlet curves are unlikely to be sufficiently low in energy to make the singlet pathway possible.^{9,17,30}

Acknowledgment. Financial support by the Jubiläumsfonds der Österreichischen Nationalbank and by the Fonds zur Förderung der wissenschaftlichen Forschung is acknowledged. Learco Minghetti and Maurizio Minghetti are gratefully acknowledged for technical assistance.

Registry No. 2-MP, 95-48-7; 3-MP, 108-39-4; 4-MP, 106-44-5; 2,6-DMP, 576-26-1; 2,4-DMP, 105-67-9; 3,5-DMP, 108-68-9; 2,4,6-TMP, 527-60-6; 2,3,5-TMP, 697-82-5; 2-MP phenoxyl radical, 3174-49-0; 3-MP phenoxyl radical, 41115-75-7; 4-MP phenoxyl radical, 3174-48-9; 2,6-PMP phenoxyl radical, 3229-35-4; 3,5-DMP phenoxyl radical, 35645-14-8; 2,4,6-TMP phenoxyl radical, 15773-14-5; 2,3,5-TMP phenoxyl radical, 125452-27-9; 1-bromobutane, 109-65-9; phenol, 108-95-2; phenoxyl radical, 2122-46-5.

(21) Myers, A. B.; Pereira, M.; Holt, P. L.; Hochstrasser, R. *J. Chem. Phys.* **1987**, *86*, 5146.

(22) Armstrong, D. R.; Cameron, C.; Nonhebel, D. C.; Perkins, P. G. *J. Chem. Soc., Perkin Trans. 2* **1983**, 569.

(23) Armstrong, D. R.; Cameron, C.; Nonhebel, D. C.; Perkins, P. G. *J. Chem. Soc., Perkin Trans. 2* **1983**, 581.

(24) Sur, A.; Johnson, P. M. *J. Chem. Phys.* **1986**, *84*, 1206.

(25) Lipert, R. J.; Colson, S. D.; Sur, A. *J. Phys. Chem.* **1988**, *92*, 183.

(26) Lipert, R. J.; Bermudez, G.; Colson, S. D. *J. Phys. Chem.* **1988**, *92*, 3801.

(27) Lipert, R. J.; Colson, S. D. *J. Phys. Chem.* **1989**, *93*, 135.

(28) Tomas, Vert, F.; Medina Casamayor, P.; Olba Torrent, A.; Monzo Mansanet, I. S. *J. Photochem. Photobiol. A* **1987**, *40*, 59.

(29) Birks, J. B. *Photophysics of Aromatic Molecules*; Wiley-Interscience: New York, 1970; p 266.

(30) Michl, J. *Top. Curr. Chem.* **1974**, *46*, 1.